2012 Ninth Conference on Computer and Robot Vision

Towards AUV Route Following Using Qualitative Navigation

Peter Vandrish
Faculty of Engineering & Applied Science
Memorial University of Newfoundland
St. John's, Canada

Andrew Vardy
Department of Computer Science
Faculty of Engineering & Applied Science
Memorial University of Newfoundland
St. John's, Canada
av@mun.ca

Peter King
Marine Environmental Research
Lab for Intelligent Vehicles
Memorial University of Newfoundland
St. John's, Canada

***Abstract*—We present a novel approach to the guidance of an autonomous underwater vehicle (AUV) along a trained route. The introduced system employs a topological route representation based on storing a sequence of side-scan sonar images captured along the route. When in following mode, image registration techniques provide the vehicle with a real-time estimate of the direction of its displacement relative to the trained route. This simplified approach to navigation sidesteps the problems inherent with maintaining a vehicle pose estimate within a global reference system, thereby allowing the vehicle to traverse a trained route without resorting to external navigation aides (e.g. GPS). Simulation results are provided which validate the proof of concept for our approach.**

***Keywords*-AUV navigation; route following; qualitative navigation; topological navigation**

I. Introduction

The system proposed here provides the capability for an autonomous underwater vehicle (AUV) to follow a previously learned route without external navigational aides. At the core of the system is an algorithm for the registration of side-scan sonar images, which has been described in previous work [1]. The approach taken is to represent the route as a sequence of nodes, each with an associated side-scan sonar image which was collected during training. This strategy is based on the notion of topological navigation pioneered in mobile robotics [2] which has also been described as *qualitative navigation* [3], [4]. The approach of qualitative navigation is to represent the environment as a set of connected places with mechanisms for travelling between places. It is quite explicit that these places are *not* represented in the same global coordinate system. These ideas have led to considerable success in recent years in allowing an outdoor mobile robot to autonomously follow a trained route, despite changes in illumination and variable terrain [4], [5]. To our knowledge, our work represents the first attempt to apply a qualitative navigation approach to the underwater domain.

In contrast to the qualitative navigation approach the current practise of AUV navigation is heavily invested in estimating the pose of the vehicle in a global coordinate system. A host of sensors and inertial measurement technologies support this goal. While on the surface, the AUV updates its position from satellite-based positioning systems such as GPS. During a dive the AUV relies on its Inertial Navigation System (INS) to estimate its acceleration and integrates this information to update its pose estimate. In the vicinity of the seabed, a Doppler Velocity Log (DVL) can be used to estimate the speed over ground, which allows for increased precision in updating the vehicle's pose. However, only the satellite-based positioning systems provide an absolute reference, and even this reference includes some error. The INS and DVL can be used to update the position estimate, but it is inevitable that it will drift from its true value. Therefore AUVs must surface periodically. The frequency of surfacing events hinge upon the accuracy of the INS. For high-end INS systems a typical value for position accuracy is 0.1% of distance travelled. Absolute position reference can also be provided to a submerged AUV by an acoustic positioning system, which may be ship-based or consist of independent transponders.

We believe it is worthwhile pursuing other navigational strategies that are less dependent upon global pose estimation. Higher-end INS systems in particular can be very expensive (in excess of $150,000). Acoustic positioning systems are also expensive, have limited range, and require some effort to install into the environment. Even if such systems are available, one must consider how to recover the AUV if they fail.

Another popular approach is to employ the technique of Simultaneous Localization and Mapping (SLAM) to acquire maps of the environment autonomously from sensor data. The application of SLAM to the underwater domain has a long history and is an area of much recent activity [6], [7]. However, the computational cost of SLAM techniques are significant and it remains unclear whether they can scale to map long routes with few self-intersections, such as have been undertaken underneath the arctic ice shelf [8].

The method described here has a number of potential applications. It could be used as an emergency return strategy for a deployed AUV. To allow for this return the vehicle would need to capture side-scan sonar images along its route during normal operations. If a fault or some other emergency condition ensued, it could traverse its course in reverse by

978-0-7695-4683-4/12 $26.00 © 2012 IEEE
DOI 10.1109/CRV.2012.63

homing in sequence from image-to-image all the way back to the launch point. Another broad area of application would be in conducting repetitive surveys of the same area of seabed—a common task in security operations and environmental monitoring. Yet another significant application area is under-ice operations where it is simply not possible for the vehicle to surface to obtain a satellite position fix. There has been considerable interest in running AUVs underneath the arctic ice shelf, in particular for the purposes of establishing territorial claims under the United Nations Convention on the Law of the Sea [8].

In our system, the AUV operates in either traning or deployment mode. In training mode, it forms images of the seabed from side-scan sonar data and stores these with a given frequency (see figure 1). In deployment mode the AUV is configured to either follow the trained route in the same direction it was collected (e.g. for surveying applications) or in the opposite direction (e.g. emergency return). We make the assumption that the AUV starts its deployment somewhere along the trained route. It will then begin a continous process of localizing itself to the nearest node along the training route and will adjust its trajectory to minimize displacement from the route and travel along it in the configured direction. In this paper we present initial results that validate the proof-of-concept for this system. The results are based on side-scan sonar images captured from a towed sensor[1]. We are currently in the process of installing a side-scan sonar and other sensors onboard Memorial University's Explorer-class AUV[2].

In the next section we describe our qualitative navigation system for autonomous route following. We then present results on towed side-scan data in section III. Finally, some concluding remarks and directions for future work are presented in section IV

II. System Design

The design of the overall qualitative navigation system is illustrated in Figure 2. The flow of information within the system is as follows:

(A) Raw scanlines are passed from the side-scan sonar to the image generation process.

(B) Heading and speed data are used by the image generation unit in the computation of scanline orientation and position.

(C) A generated side-scan image is forwarded on for the purposes of image registration and localization.

(D) The localization unit uses the results from the registration of the current image with those in the database to aid in the process of localization.

(E) Localization compares the current (sensed) image with the database images obtained during the training phase.

[1]Data kindly provided by EdgeTech, Wareham, MA, USA.

[2]Manufactured by International Submarine Engineering Ltd., Port Coquitlam, BC, Canada.

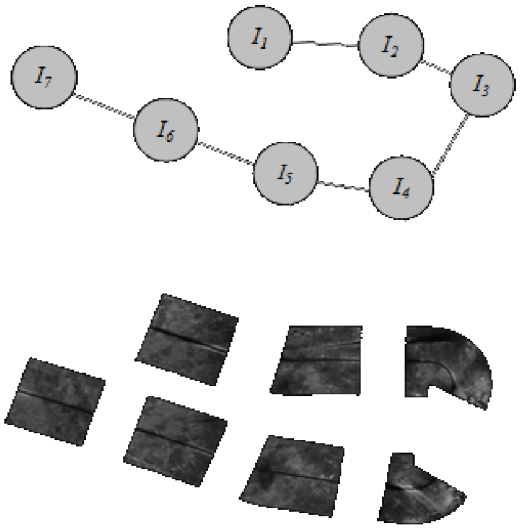

Figure 1. The representation of a topological route through the use of side-scan sonar images.

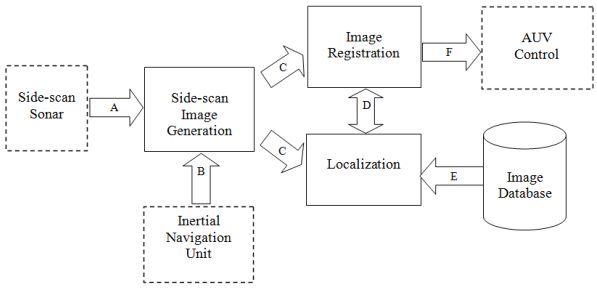

Figure 2. A block diagram representation of the overall qualitative navigation system.

(F) The transformation parameters resulting from the image registration and localization processes are passed along to the AUV control module.

The overall outputs of the system are transformation parameters which provide an estimate of the vehicle's displacement and orientation relative to the route. These parameters can then be used by an AUV control unit in deciding how to set a new course. Perhaps the most straightforward approach would be to use the transformation parameters to compute a new waypoint. This approach is possible because the Explorer AUV's control software has the capability to set new waypoints on-the-fly and home towards them autonomously. Although an important consideration for practical implementation, we do not yet have the means to evaluate different control strategies on

the AUV. Therefore the investigation of control strategies is left for future work and we focus instead on the problem of computing the relative transform between the AUV and the route.

A. Side-scan Image Generation

A side-scan sonar emits acoustic pings and records the time and intensity of response over an integration window. The result is that each ping samples the seabed along a line orthogonal to the vehicle's direction of travel. The data recorded from each ping is known as a *scanline*. The area sampled increases in size with distance from the sensor, and there are a number of other factors and corrections that must be accounted for when analyzing side-scan sonar data [9]. Commercial software packages are available to generate a two-dimensional side-scan image by appropriately combining the one-dimensional scanlines generated from each ping. However, we require this process to be executed in real-time without user intervention onboard the AUV.

There is insufficient space to describe the complete side-scan image generation process here. The core of the process is to combine into one raster image the scanlines collected from each ping, while also applying the appropriate corrections (e.g. correcting for attenuation of the signal with distance from the sensor). Writing these scanlines into the appropriate positions of the image requires information about the relative change in the AUV's pose. In our case, we generate image tiles that combine a constant number of scanlines into one image. Any deviations of the vehicle from a straight course will result in data from multiple scanlines being written to the same raster location. Sophisticated interpolation schemes are required to combine this data appropriately. Some examples of the image tiles generated by this process can be seen in figures 6 and 8.

B. Image Registration

The image registration procedure is based on extracting SIFT keypoints [10] and utilizing RANSAC [11] to arrive at a subset of the keypoints which are used to estimate a two-dimensional rigid body transform between the sensed and reference images. We previously compared this approach with other image registration techniques including mutual information, phase correlation, and a method based on the correlation between log-polar transformed images [1]. The performance of SIFT and phase correlation were similar. We have adopted SIFT over phase correlation so that the sonar images themselves can be discarded once keypoints have been extracted. The keypoints typically consume less storage space than the images thereby mitigating storage space concerns as a constraint on the range of our technique.

We make the assumption that the AUV will operate at constant depth. The desired depth value can be easily stored as a characteristic of the route. This assumption simplifies the geometry and allows us to consider only two-dimensional transforms in the image registration process.

C. Localization

The localization process ties the entire system together. It provides an estimate of the vehicle's location along the route and attempts to maintain that estimate even when the vehicle becomes temporarily lost. This is accomplished through the use of recursive Bayesian estimation [12]. The vehicle is assumed to be travelling in the configured direction along the route (either in the same direction as in training or opposite).

1) Bayes Filter: Recursive Bayesian estimation is a process for estimating the probability distribution of a system over its state-space. In our case, the system is the AUV and its state-space corresponds to topological position along the trained route. A single position is represented simply as a node index. Bayes filter allows the AUV to continuously update its state estimate based on the most recently acquired side-scan image. The filter consists of two parts: prediction and innovation. A motion model is used in the prediction step to model the vehicle's recent motion. In the innovation step the AUV will refine the current belief estimate according to sensory input.

The granularity of the position estimate is determined by the number of nodes along the trained route. It is possible for a sensed image to be partially contained within two adjacent reference images, in which case the probability mass is expected to be distributed among them in the measurement function. The Bayesian network shown in Figure 3 represents the process of updating the vehicle's unknown position $\mathbf{w}_k$ at instant k based on the observation $\mathbf{z}_k$ and motion estimate $\mathbf{r}_k$. The vehicle's belief that it is at

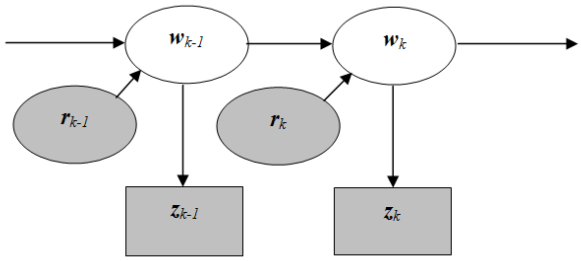

Figure 3. An example of a general Bayesian network for vehicle localization.

some position $\mathbf{w}_k$ is denoted by a belief function:

$$bel(\mathbf{w}_k) = p(\mathbf{w}_k|\mathbf{z}_{1:k}, \mathbf{r}_{1:k}), \quad (1)$$

where the subscript $1:k$ represents all current and past observations and motion updates. The belief function bel is initialized to a uniform distribution which represents the vehicle being completely uncertain with respect to its

position. Upon applying the motion model to the previous belief function the prediction function is then obtained:

$$\overline{bel}(\mathbf{w}_k) = \sum_{\mathbf{W}_{k-1}} p(\mathbf{w}_k|\mathbf{r}_k, \mathbf{w}_{k-1}) bel(\mathbf{w}_{k-1}) \quad (2)$$

where $p(\mathbf{w}_k|\mathbf{r}_k, \mathbf{w}_{k-1})$ is the probability that the vehicle arrived at position $\mathbf{w}_k$ given that it was previously at position $\mathbf{w}_{k-1}$ and underwent motion $\mathbf{r}_k$. The prediction function is an intermediate belief about the vehicle's position without taking the current observation into account. The innovation step allows the prediction function to be refined according to the current observation and the prediction function:

$$bel(\mathbf{w}_k) = \mu p(\mathbf{z}_k|\mathbf{w}_k)\overline{bel}(\mathbf{w}_k), \quad (3)$$

where $p(\mathbf{z}_k|\mathbf{w}_k)$ expresses the probability that the most current observation is consistent with $\mathbf{w}_k$, also known as the measurement model, and μ is simply a normalizing constant which constrains the sum of the probability mass under the resulting belief function to be equal to one:

$$\mu = \frac{1}{\sum_{\mathbf{W}_k} p(\mathbf{z}_k|\mathbf{w}_k)\overline{bel}(\mathbf{w}_k)} \quad (4)$$

The process described here is reiterated each time a new observation is made. The probability mass within the belief function will eventually converge on the vehicle's true position as long as the vehicle remains in close proximity to the route and some sequence of distinguishing features is observed. The strongest estimate of the vehicle's position is used to determine position. Image registration is then applied to relate the current image to the corresponding training image. The resulting transformation parameters will be used to guide the vehicle back onto the route. If there is no sufficiently strong position estimate, a default navigation strategy may be assumed. Currently, we are accepting as a default strategy that if the vehicle does not have a strong estimate of its position it will continue in the direction suggested by its most recent estimate.

2) Motion Model: For our purposes a very simple motion model is used. It is derived from the assumption that the vehicle is indeed travelling along the route at constant speed in the configured direction. Under this assumption, $\mathbf{r}_k$ in equations 1 and 2 can be ignored and the motion model is reduced to $p(\mathbf{w}_k|\mathbf{w}_{k-1})$. We are anticipating that the vehicle will traverse from node to node in linear succession along the route and that there may only be very minor deviations from this pattern. As such, the current definition of the motion model is constructed similar to the one proposed in [13]:

$$p(\mathbf{w}_k|\mathbf{w}_{k-1}) = \frac{1}{\beta_{\mathbf{W}}} e^{-dist(\mathbf{w}_{k-1}, \mathbf{w}_k)/\sigma^2_{\mathbf{W}}} \quad (5)$$

where $dist(\mathbf{w}_1, \mathbf{w}_2)$ corresponds to a measurement of the distance between two places which is approximated by considering the number of place transitions between the nodes $\mathbf{w}_1$ and $\mathbf{w}_2$ on the topological map, and $\sigma^2_{\mathbf{W}}$ is the measured variance of the distances between adjacent nodes determined prior to deployment. β is a normalization constant.

This motion model is limited in that it does not take the actual movements of the vehicle into consideration. In the future, it will be extended to accept input from the AUV's INS so that we can compare the actual distance travelled with stored relative movements between node locations.

3) Measurement Model: We have devised a measurement model which utilizes the same similarity metric used by the SIFT/RANSAC method for image registration. This registration method measures the similarity between a transformed sensed image and a reference image by counting the number of inliers resulting from the transformation. Those keypoints which are in agreement with the transformation parameters are called inliers. Let the similarity function be denoted by

$$N_{in} = S(I_S, I_R), \quad (6)$$

where the function returns the number of inliers N_{in} found when registering sensed image I_S to reference image I_R. The database D of reference images along the route is as follows:

$$D = \{I_{R1}, I_{R2}, I_{R3}, ...\}. \quad (7)$$

We can compute a set of similarity functions over D

$$F_{inliers} = \{S(I_S, I_{R1}), S(I_S, I_{R2}), ...\} \quad (8)$$

The measurement model, which is a probability mass function, is approximated by determining the relative frequency of each result within the set of similarity results:

$$p(\mathbf{z}_k|\mathbf{w}_k) = \frac{F_{inliers}}{\sum_i F_{inliers}(i)} \quad (9)$$

III. Results

A. Experimental Setup

At the time when these results were developed the MUN Explorer AUV was not yet outfitted with the side-scan sonar required for this work. We therefore utilized data collected by a towed side-scan sonar collected off the port of Southhampton, UK. The data consists of two partially overlapping track lines, as shown in Figure 4, corresponding to two independent runs over a particular region of seabed. GPS information is included as meta-data. The longer track line in Figure 4 is taken as the simulated training route for the system. A total of 15 image tiles, each consisting of 500 scanlines, were obtained along this route. The shorter track (shown in red) is taken as the simulated deployment route. A total of 8 images were obtained along the deployment route. The direction of travel for both routes is shown in the figure.

The objective of the experiments described here are to validate our localization strategy, the ability of our image

(a) Overhead view from Google Maps

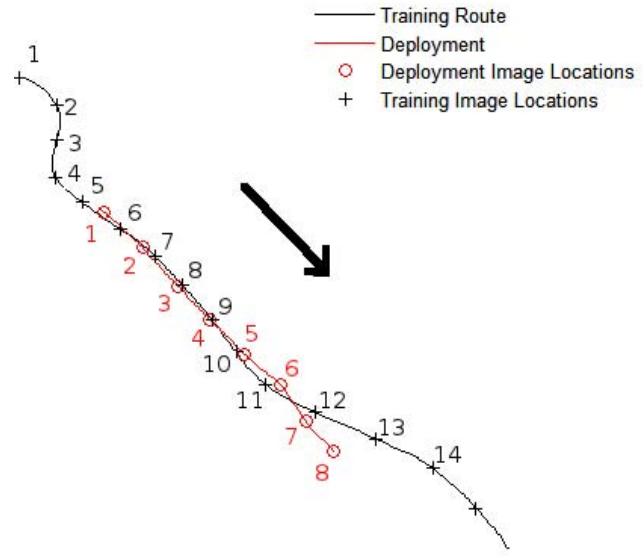

(b) Labelled routes

Figure 4. Two routes used for system validation. Data obtained off of the coast of Southampton, UK. The longer track is considered the training route. The shorter red track is the deployment, or testing route.

registration procedure to determine the correct local transform, and finally to combine localization and local transform to determine on which side of the route the vehicle lies.

B. Localization

We begin by considering the measurement model. Figure 5 provides a graphical representation of the probabilities of obtaining the given sensed image along each trained position of the route. As mentioned in section II-C3 the measurement model is based on the registration strength of the current sensed image with each of the trained images. Most of the probability mass is focused along a diagonal which starts at reference image 6. As can be observed from Figure 4, the initial position of the vehicle is between two reference nodes; 5 and 6. For sensed positions 1-6, the peak of the probability function shifts along as expected. However, a dropoff occurs at sensed image 6 and the measurement model (on its own) incorrectly predicts position for sensed images 6-8. This is due to the fact that the swath width is fairly narrow and the vehicle is increasingly deviating from the training route, so overlapping coverage is limited and devoid of content that would otherwise produce a strong registration. Figure 6 shows sensed image 6 and reference image 11, a pair for which our method fails to find sufficient correspondences.

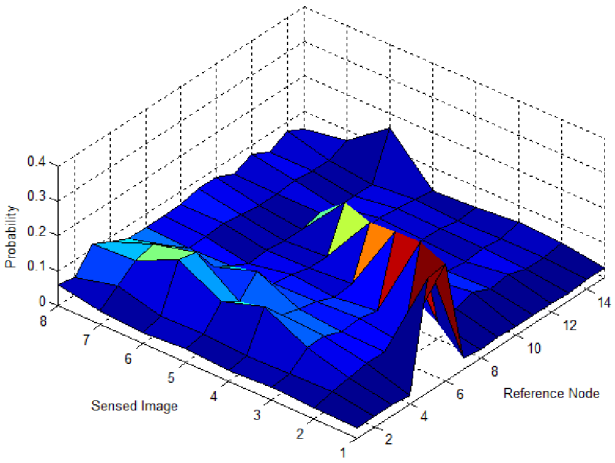

Figure 5. Measurement probability function $p(\mathbf{z}_k|\mathbf{w}_k)$ dependent on sensed image input.

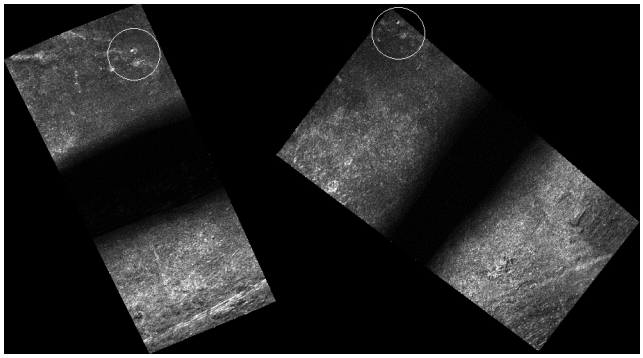

Figure 6. Sensed image 6 (left) and training image 11 (right) result in a weak registration. The circled regions are manually identified commonalities.

The belief function, which incorporates both motion and measurement models, can be evaluated similarly. Figure 7 shows a graphical representation of the belief function as

it evolves for each new sensed image from 1-8. For sensed images 1-5 the peak in probability tracks along correctly. For sensed images 6-8 the inaccuracies described above are inherited by the belief function and a clear drop in peak intensity is observed. However, the peak in the belief function is closer to the true value than it was for the measurement model alone. In fact, the peak in the belief function is still coincident with the correct location for images 6 and 7 (reference images 11 and 12). Only for sensed image 8 is the peak located incorrectly (at reference image 13 as opposed to 14). To model the uncertainty of the vehicle, we have calculated the entropy in the belief function each time a new sensed image is obtained. These entropy values are given in table I. Initially, uncertainty is high because the belief function was initialized to a uniform distribution which results in a direct copying of probability from the measurement model. The uncertainty then trends downwards until we hit the difficult patch from sensed images 6-8.

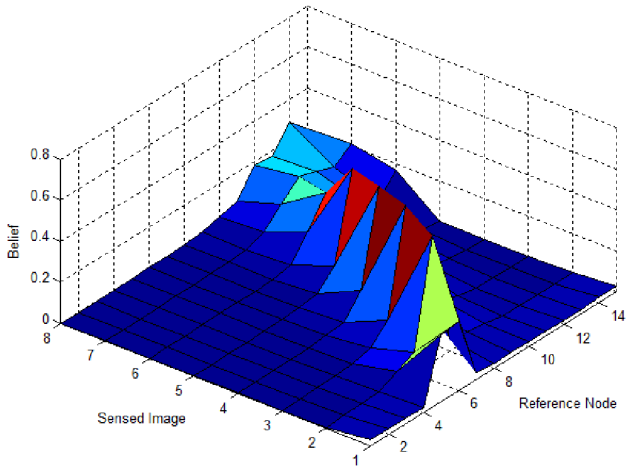

Figure 7. Belief function $bel(\mathbf{w}_k)$ dependent on sensed image input.

Table I
LOCATION ESTIMATE OBTAINED FROM THE BELIEF FUNCTION.

Sensed Image	Location Estimate (Training Node)	Entropy
1	6	1.97
2	7	1.52
3	8	1.40
4	9	1.47
5	10	1.55
6	11	1.94
7	12	1.92
8	14	1.82

We can see that, through the use of the Bayes filter for localization, along with the proposed motion and measurement models, our system has the ability to maintain an accurate estimate of its location even while the measurement model returns a weak estimate. We believe the difficulty that occurs for sensed images 6-8 is due to the increasing deviation of the vehicle from its trained route. This decreases the overlapping area between the images. Also, the generally homogeneous texture in this area of seabed makes localization difficult (see figure 6).

C. Local Transform

Image pairs with sufficient overlapping content produce excellent registration results. Figure 8 provides an example illustrating how the coordinate system of reference image 6 relates to sensed image 1. Figure 6 provides an example where the correct transformation between images could not be found.

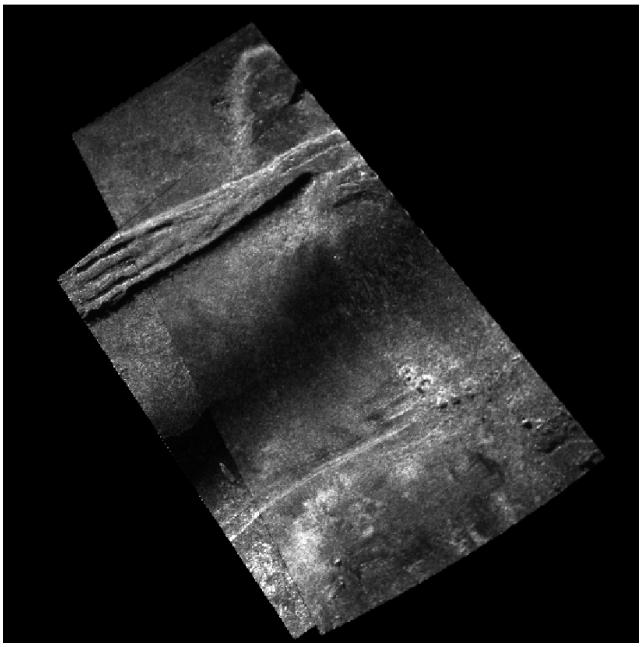

Figure 8. The registration of sensed image 1 with reference image 6.

Figure 9 shows the local transformations computed along the route, as well as providing a graphical depiction of the entropies given in table I. It can be seen that for sensed images 1-5 the transforms are all approximately correct, but that for images 6-8 they are incorrect. It is important to note that the arrows depicted in this figure show the spatial relationships to the most similar positions along the training route and should not be taken as direct instructions for piloting the AUV.

D. Route Side Determination

By combining localization with image registration we can determine on which side of the route the vehicle lies. In figure 10 the translation vector from the local transform is projected onto the vehicle's heading vector and then normalized to constant length. For images 1-6 these vectors

point orthogonally in the direction of the route, indicating which steering direction should be chosen. However, for positions 7 and 8 the estimate is incorrect.

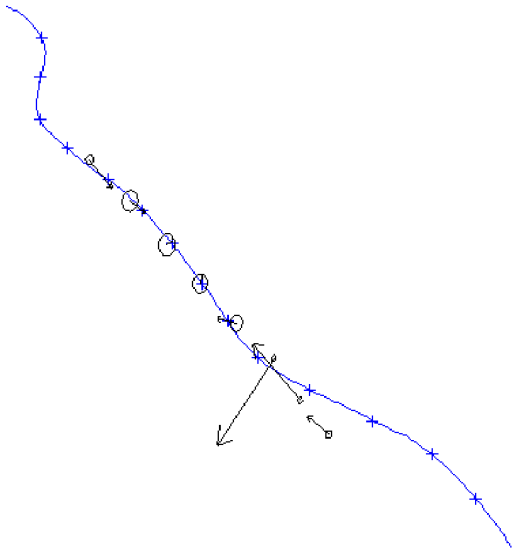

(a)

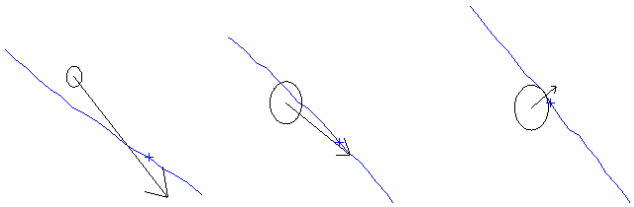

(b) Close ups for sensed images 1-3

Figure 9. The local transformations computed along the route. Arrows indicate the relative direction of translation as a result of image registration. Circle radius is proportional to the entropies provided in table I, the larger the radius the more certain the vehicle is of its location. Circle locations correspond to the true locations of the vehicle.

E. Discussion

For 7 out of 8 positions along the route, our localization system was able to track its position, and for 6 out of 8 positions it was able to make the correct route-side determination. For the positions where route-side was estimated incorrectly, we saw a high entropy value indicating uncertainty. Therefore, we have some confidence that the system described here could be developed further to offer route guidance where possible, but could also be designed to maintain the current course (or switch to some other strategy) when localization uncertainty reaches a high level.

These simulation results, however preliminary, show that underwater navigation by an AUV is possible even in the absence of external localization aides or by referring to its location within a global frame of reference.

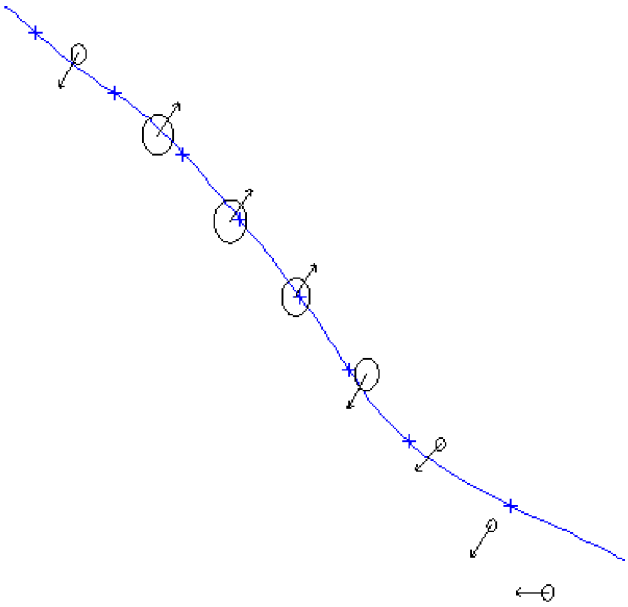

Figure 10. Indication of the location of the route relative to the vehicle's current heading.

IV. Conclusions

Our intent has been to produce a system for underwater navigation which does not rely on global pose estimation. Current strategies for AUV navigation rely on external navigation aides such as GPS which may require the vehicle to surface periodically, therefore limiting the time spent underwater. The system proposed here is suitable for routine surveying or monitoring applications where the vehicle is required to follow a trained route precisely and for an extended period. Instead of attempting to maintain an estimate of the vehicle's location in a global reference frame, the vehicle needs only to determine its position along the route and to determine on which side of the route it lies.

Simulation results show that our system does indeed provide the vehicle with an estimate of its location and a navigation vector indicative of the course correction required to steer the vehicle toward the route.

It is clear, however that much work remains to be done. We feel that the restriction to constant-depth route following can be relaxed, especially considering the availability of scale-invariant image registration techniques. In this paper we adopted SIFT features for both image registration and similarity measurement. However, we intend to investigate other scale-space detectors which have been reported to improve upon SIFT's accuracy and computational cost [14], [15]. We also wish to incorporate a motion model that

accounts more accurately for the vehicle's recent trajectory. More investigation is required into a control strategy that would bring a displaced vehicle back to the route in an efficient manner (for example, by selecting a later point along the route as a waypoint). We observed some degree of ambiguity in the measurement model, which may be addressed by other image matching techniques such as histogram matching and textural analysis. Our most immediate challenge is to deploy and test this system on a working AUV.

ACKNOWLEDGMENT

This work is part of the REALM project at Memorial University which is supported by the Atlantic Canada Opportunities Agency (ACOA), Memorial University of Newfoundland, Research & Development Corporation of Newfoundland and Labrador, and Fugro Geosurveys Ltd. of St. John's, NL, Canada. We also wish to thank Fugro Geosurveys Ltd. and EdgeTech Ltd. of Wareham, MA, USA for sharing their side-scan sonar datasets and working with us in the collection of those datasets.

REFERENCES

[1] P. Vandrish, A. Vardy, D. Walker, and O. Dobre, "Side-scan sonar image registration for AUV navigation," in *IEEE Symposium on Underwater Technology*, 2011.

[2] B. Kuipers and Y.-T. Byun, "A robot exploration and mapping strategy based on a semantic hierarchy of spatial representations," *Journal of Robotics and Autonomous Systems*, vol. 8, pp. 47–63, 1991.

[3] D. Dai and D. Lawton, "Range-free qualitative navigation," in *IEEE ICRA*, 1993.

[4] Z. Chen and S. Birchfield, "Qualitative vision-based path following," *IEEE Transactions on Robotics*, vol. 25, no. 3, pp. 749–754, 2009.

[5] A. Zhang and L. Kleeman, "Robust appearance based visual route following for navigation in large-scale outdoor environments," *The International Journal of Robotics Research*, vol. 28, no. 3, pp. 331–356, 2009.

[6] H. Johannsson, M. Kaess, B. Englot, F. Hover, and J. Leonard, "Imaging sonar-aided navigation for autonomous underwater harbor surveillance," in *IEEE/RSJ International Conference on Robots and Systems (IROS)*, 2010.

[7] A. Mallios, P. Ridao, D. Ribas, F. Maurelli, and Y. Petillot, "EKF-SLAM for AUV navigation under probabilistic sonar scan-matching," in *IEEE/RSJ International Conference on Robots and Systems (IROS)*, 2010.

[8] T. Crees, C. Kaminski, J. Ferguson, J. M. Laframboise, A. Forrest, J. Williams, E. MacNeil, D. Hopkin, and R. Pederson, "Preparing for unclos an historic auv deployment in the canadian high arctic," in *MTS/IEEE OCEANS*, 2010.

[9] P. Blondel, *The Handbook of Sidescan Sonar*. Springer Praxis, 2009.

[10] D. Lowe, "Distinctive image features from scale-invariant keypoints," *International Journal of Computer Vision*, vol. 60, no. 2, pp. 91–110, 2004.

[11] M. A. Fischler and R. C. Bolles, "Random sample consensus: A paradigm for model fitting with applications to image analysis and automated cartography," *Communications of the ACM*, vol. 24, pp. 381–395, 1981.

[12] S. Thrun, W. Burgard, and D. Fox, *Probabilistic Robotics*. MIT Press, 2005.

[13] T. Goedemé, M. Nuttin, T. Tuytelaars, and L. Van Gool, "Omnidirectional vision based topological navigation," *International Journal of Computer Vision*, vol. 74, no. 3, pp. 219–236, 2007.

[14] H. Bay, A. Ess, T. Tuytelaars, and L. V. Gool, "SURF: Speeded up robust features," *Computer Vision and Image Understanding*, vol. 110, no. 3, pp. 346–359, 2008.

[15] M. Ebrahimi and W. Mayol-Cuevas, "SUSurE: Speeded up surround extrema feature detector and descriptor for realtime applications," in *Computer Vision and Pattern Recognition Workshops*, 2009.